Journal of Medicinal Chemistry

Article

pubs.acs.org/jmc

The Effect of Pro^2 Modifications on the Structural and Pharmacological Properties of Endomorphin-2

Attila Borics,[†] Jayapal R. Mallareddy,[†] István Timári,[‡] Katalin E. Kövér,[‡] Attila Keresztes,[†] and Géza Tóth*[,†]

[†]Institute of Biochemistry, Biological Research Center of the Hungarian Academy of Sciences, P.O. Box 521, H-6701 Szeged, Hungary

[‡]Department of Chemistry, University of Debrecen, P.O. Box 21, H-4010 Debrecen, Hungary

Supporting Information

ABSTRACT: Endomorphins (EM-1 and EM-2) are selective, high affinity agonists of the μ-opioid (MOP) receptor, an important target in pain regulation. Their clinical use is impeded by their poor metabolic stability and limited entry to the central nervous system. In this study, the Pro^2 residue of EM-2 was modified systematically through substitution by hydroxyproline (Hyp), (*S*)-β-homoproline (βPro), 2-aminocyclopentene-1-carboxylic acid (ΔAcpc), or 2-aminocyclohexene-1-carboxylic acid (ΔAchc) to obtain stable MOP active compounds. Both Hyp^2 and βPro^2 substitution decreased receptor affinity. Analogues incorporating alicyclic β-amino acids exhibited diverse receptor binding properties, depending on the configuration of the substituent side-chain. (1*S*,2*R*)ΔAcpc^2−EM-2 was shown to have MOP affinity and selectivity comparable to those of EM-2 and proved to act as agonist while being resistant to proteolysis. NMR and molecular dynamics (MD) studies revealed that bent backbone structures are predominant in the most potent analogues, while their presence is less pronounced in ligands of lower receptor affinity.

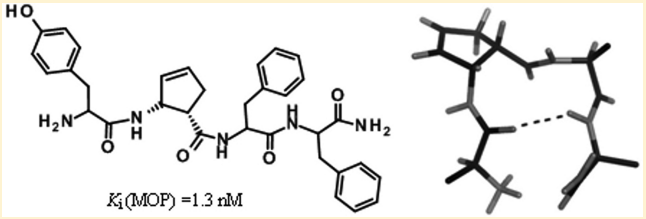

INTRODUCTION

Opioid receptors are members of the superfamily of G-protein-coupled receptors (GPCR). Three classical types of opioid receptors have been identified based on pharmacological and behavioral observations, namely μ-, δ-, and κ-receptors (MOP, DOP, and KOP, respectively). These receptors mediate the actions of opiate alkaloids and opioid peptides and take part in a variety of biological processes, including pain perception and modulation.[1] Among those, MOP receptors are targeted in the search for new drugs to suppress chronic pain.[2] Endomorphin-1 (EM-1, H-Tyr-Pro-Trp-NH_2) and endomorphin-2 (EM-2, H-Tyr-Pro-Phe-Phe-NH_2) were initially isolated from bovine[3] and later from human brain cortex.[4] These peptides are the putative endogenous ligands of the MOP based on their high affinity and exceptional selectivity. Therefore they became important models in analgesic research. Analgesic effects occur within the central nervous system (CNS), so peptides should be able to cross the blood−brain barrier (BBB) intact. However, exogenous application of EMs is limited by short duration of action, low in vivo efficacy,[5] poor metabolic stability,[6] and inability to cross the BBB.[7] Considering EMs as potential therapeutic drugs, it is essential to enhance their resistance to enzymatic degradation and ability to enter the CNS. This could be accomplished by chemical modifications of EM structure.[8−10] However, the preservation of pharmacological properties of EMs in the modified analogues necessitates full understanding of the structural requirements of MOP binding and activation. A significant amount of effort was devoted in the past decade to the investigation of structure−activity relationships of EMs and their analogues,[8−11] and several bioactive structure models were proposed.[12−19] Approximate distances between pharmacophore groups were first proposed to define their spatial arrangement required for binding to the MOP.[12] Later, a more detailed bioactive structure model was provided to define exact backbone and side chain conformations which furnish the optional spatial arrangement of the first (Tyr^1) and second (Phe^3) pharmacophore side chains.[13] Notable emphasis was put on the role of *cis*−*trans* isomerization of the peptide bond preceding Pro^2 in EMs. However, this structural property was proved to be less important, as exclusively *cis*[15] and exclusively *trans*[20,21] EM analogues were both shown to bind to the MOP with high affinity. Despite several minor discrepancies, most of the recent pharmacophore models agree in proposing the importance of bent backbone structure.[13,16,18,19] All such pharmacophore models are deducted from intrinsic structural tendencies modeled or observed in isolated molecules in solution or from molecular docking studies using theoretical receptor structures and binding site models. Even though X-ray crystallographic structure of the μ-opioid receptor was reported earlier this year[22] and there are several points of agreement in previous independent suggestions, the design of a MOP-agonist peptide with pharmaceutical properties appropriate for therapeutic application remains a challenge.

Received: June 14, 2012
Published: September 10, 2012

It was shown earlier that modifications of Pro^2 in the sequence of EMs could yield proteolytically stable, yet MOP-active compounds,[15,20,23−25] as such modifications do not alter the main pharmacophore groups.[12,26,27] Such modifications included the substitution of Pro^2 with 1,2,3,4-tetrahydroisoquinoline-3-carboxylic acid (Tic),[23] pseudoprolines (ΨPro),[15] six-membered heterocyclic rings, such as piperidine-2-, 3-, and 4-carboxylic acids ((*S*)-Pip, (*R*)-Nip, and Inp, respectively),[24] four-membered azetidine rings (Aze, 3Aze),[25] and alicyclic *β*-amino acids (Acpc, 2-aminocyclopentane-1-carboxylic acid; Achc, 2-aminocyclohexane-1-carboxylic acid) (Figure 1).[20]

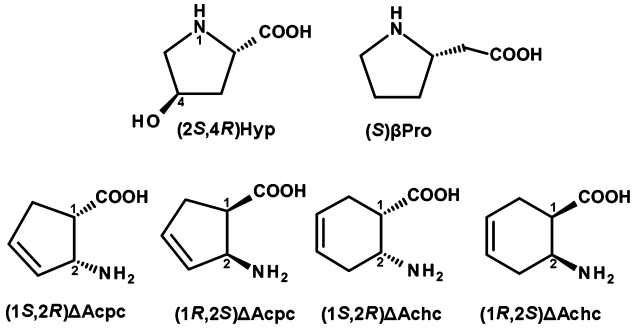

Figure 1. Structures of unnatural amino acids incorporated in position 2 of endomorphin-2.

Systematic review of these results suggests the importance of ring structure and size in determining the bioactivity of the ligands. According to the general view, the second residue in MOP ligands act as a stereochemical spacer, responsible for the three-dimensional orientation of pharmacophore groups.[27] The study of EM analogues in which Pro^2 was replaced by alicyclic *β*-amino acids revealed that the configuration of the side chain in that position affects secondary structure and therefore has a dramatic effect on receptor binding properties.[20] The results also suggest that the second residue of MOP ligands may take part in receptor−ligand interactions as well, although such possibilities have not yet been fully explored. The hydroxylation of proline residues by prolyl 4-hydroxylase to form (2*S*,4*R*)-4-hydroxyproline (Hyp) is a common post-translational modification in humans. The presence of a polar −OH group in the Hyp side chain may alter protein conformation and affect protein−protein interactions.[28] Substitution of Pro^2 by Hyp in EM-2 was shown to decrease MOP affinity relative to the parent peptide, but no specific data for the selectivity and structural properties of the resultant analogue were given.[29] Insertion of (*S*)-*β*-homoproline (*β*Pro) in EM-2 yielded an analogue with decreased MOP binding affinity and slightly enhanced proteolytic stability against enzymatic degradation.[30]

Here, a detailed pharmacological characterization, enzymatic degradation studies, and structural analysis of a set of synthetic EM-2 analogues, systematically modified in the second position of the sequence, is presented. By the incorporation of Hyp^2, *β*Pro^2, ΔAcpc^2, and ΔAchc^2, the role of a polar side chain group, the structural effects of the elongation of the backbone by $-CH_2-$ group, and the significance of the tertiary amide moiety in the backbone is investigated. Furthermore, structural analysis of ΔAcpc^2−EM-2 and ΔAchc^2−EM-2 was done to reveal how modified side chain ring puckering properties affect secondary structure and MOP affinity. Besides its role as a stereochemical spacer, the possibility of a more significant involvement of Pro^2 in receptor−ligand interactions is also examined.

RESULTS

Synthesis. Analytical properties of the synthetic analogues are summarized in Table 1. High resolution mass spectrometry (HRMS) experiments confirmed the mass identity of all synthesized compounds. RP-HPLC analyses of the final purified products indicated purity of at least 96% in all cases. Diastereomers of compounds **4**−**7** were successfully separated by RP-HPLC after GITC derivatization, and their identities were confirmed by comparison of their retention times to those of *β*-amino acid containing standards.[31,32] The ratio of the crude diastereomeric peptides was found to be nearly 1:1 with respect to the (1*S*,2*R*)ΔAcpc^2/ΔAchc^2 and (1*R*,2*S*)ΔAcpc^2/ΔAchc^2-containing EM-2 analogues.

Biological Evaluation. Inhibitory constants (K_i) and selectivities (K_i^{δ}/K_i^{μ}) of the new analogues and the parent ligand determined by means of radioligand binding assays are listed in Table 2. The rank order of potency of all compounds measured against [^{3}H]DAMGO was as follows: **4** > **1** > **6** > **3** > **2** > **5** > **7**. The new EM analogues displaced the radiolabeled MOP and DOP ligands in a concentration dependent manner. As expected, diverse pharmacological activity profile was observed for the newly synthesized EM-2 derivatives. Incorporation of Hyp^2 (compound **2**) resulted in an order of magnitude decrease in the affinity to the MOP (K_i = 44 nM), compared to EM-2, similarly to a previous study where binding affinity were measured using the general opioid antagonist naloxone in crude rat brain membrane preparations.[29] Furthermore, compound **2** did not show detectable binding to the DOP. Insertion of *β*Pro^2 (compound **3**) resulted in

Table 1. RP-HPLC, TLC, and Mass Spectrometry Data of Endomorphin Analogues

			TLC[a]				
no.	peptide	crude yield (%)	R_f (A)	R_f (B)	HPLC[b] (k')	monoisoopic mass calcd	measured mass
1	Tyr-Pro-Phe-Phe-NH_2	80	0.57	0.76	1.78	571	572.24[c]
2	Tyr-Hyp-Phe-Phe-NH_2	72	0.58	0.91	1.49	587.2686	588.2764
3	Tyr-*β*Pro-Phe-Phe-NH_2	75	0.43	0.67	1.97	585.2796	586.2874
4	Tyr-(1*S*,2*R*)ΔAcpc-Phe-Phe-NH_2	73	0.56	0.82	2.51	583.2779	584.2857
5	Tyr-(1*R*,2*S*)ΔAcpc-Phe-Phe-NH_2	73	0.67	0.71	1.71	583.2747	584.2825
6	Tyr-(1*S*,2*R*)ΔAchc-Phe-Phe-NH_2	79	0.50	0.76	2.65	597.2559	598.2637
7	Tyr-(1*R*,2*S*)ΔAchc-Phe-Phe-NH_2	79	0.68	0.67	1.99	597.2715	598.2793

[a]Retention factors on silica gel 60 F_{254} plates. Solvent systems: (A) 1-butanol/acetic acid/water (4:1:1); (B) acetonitrile/methanol/water (4:1:1). [b]Capacity factors for Altima HP C_{18} (25 cm × 0.46 cm, d_p = 5 μm) column. The gradient was from 20% up to 60% ACN during 20 min, at a flow rate of 1 mL/min, λ = 216 nm. [c]Mass was measured using MS/MS.

dx.doi.org/10.1021/jm300836n | J. Med. Chem. 2012, 55, 8418−8428

Table 2. Opioid Receptor Binding Affinities and Selectivities of EM Analogues, Measured in Rat Brain Membrane Preparation

		inhibitory constants		selectivity
no.	peptide	K_i^{μ} (nM)[a]	K_i^{δ} (nM)[b]	K_i^{δ}/K_i^{μ}
1	Tyr-Pro-Phe-Phe-NH_2	1.4 ± 0.1	8495 ± 374	6068
2	Tyr-Hyp-Phe-Phe-NH_2	44 ± 3.4	>10000	
3	Tyr-βPro-Phe-Phe-NH_2	27 ± 2.6	>10000	
4	Tyr-(1*S*,2*R*)ΔAcpc-Phe-Phe-NH_2	1.3 ± 0.2	9935 ± 1218	7642
5	Tyr-(1*R*,2*S*)ΔAcpc-Phe-Phe-NH_2	2158 ± 213	>10000	
6	Tyr-(1*S*,2*R*)ΔAchc-Phe-Phe-NH_2	2.6 ± 0.2	1028 ± 121	395
7	Tyr-(1*R*,2*S*)ΔAchc-Phe-Phe-NH_2	2299 ± 372	>10000	

[a][^{3}H]DAMGO (K_d = 0.5 nM) was used as radioligand for the μ-opioid receptor. [b][^{3}H]Ile^{5,6}deltorphin-2 (K_d = 2.0 nM) was used as radioligand for the δ-opioid receptor. K_i values were calculated according to the Cheng–Prusoff equation: $K_i = EC_{50}/(1+[\text{ligand}]/K_d)$, where the shown K_d values were taken from literature data.[1] Data are expressed as means ± SEM, $n \geq 3$.

receptor affinity in the range of that of Hyp^2–EM-2 (K_i = 27 nM), confirming previous observations.[30] Receptor binding results of unsaturated alicyclic β-amino acid containing analogues (compounds **4**–**7**) are comparable with those of the respective saturated variants.[20] Compound **4** bound with similar affinity (K_i = 1.3 nM) and selectivity to the MOP relative to EM-2. Furthermore, the configuration of ΔAcpc and ΔAchc residues affected binding properties essentially the same way as that observed in the case of Acpc^2/Achc^2–EM-2 analogues previously because the inhibitory constants of compounds **5** and **7** were found to be 3 orders of magnitude higher than those of compounds **4** and **6**.

On the basis of the competitive receptor binding assay results, the most potent analogues were selected for [^{35}S]GTPγS functional binding assay. Potency (EC_{50}) and efficacy (E_{max}) values are compared to those of the full MOP agonist compound DAMGO, and the results of the ligand-stimulated [^{35}S]GTPγS assays are summarized in Table 3. The

Table 3. Summary of [^{35}S]GTPγS Functional Assay Results of Selected EM Analogues in a Rat Brain Membrane Preparation[a]

peptides	EC_{50} (nM)	E_{max} (%)
DAMGO	485 ± 24	173 ± 4
1	383 ± 12	154 ± 6 ns
2	66 ± 38	148 ± 9 ns
3	845 ± 109	116 ± 2***[b]
4	345 ± 12	170 ± 12 ns
6	1024 ± 3	162 ± 6 ns

[a]Sigmoid dose–response curves of the listed peptides were determined as described in the Experimental Section. EC_{50} and E_{max} values were calculated by using the sigmoid dose–response fitting option of the GraphPad Prism software. Data are expressed as the % stimulation of the basal activities, i.e., the binding in the absence of peptides, which was defined as 100%. Data are means ± SEM, $n \geq 3$, each performed in triplicate. [b]*** = $P < 0.001$ as assessed by one-way ANOVA and Bonferroni's post hoc test (compared to DAMGO).

rank order of efficacy (E_{max}) values is as follows: DAMGO > **4** > **6** > **1** > **2** > **3**. All of the analogues demonstrated dose-dependent increases in [^{35}S]GTPγS binding assays. The potencies and efficacies measured for DAMGO and EM-2 were in reasonable agreement with earlier results.[33,34] All selected analogues stimulated G-protein activation moderately. Compounds **2** and **3** were shown to act as a weak partial agonist (E_{max} = 148%) and partial antagonist (E_{max} = 116%), respectively. Interestingly, compound **3** had the highest potency (EC_{50} = 66 nM), higher than it was found previously in guinea pig ileum and mouse vas deferens tissue bioassays.[30] Efficacies measured for EM-2 analogues containing unsaturated alicyclic β-amino acids were similar to data obtained previously for Acpc^2 and Achc^2-substituted EM-2 analogues.[20] The highest efficacy value among all analogues was measured for compound **4** (E_{max} = 170%) comparable to that of MOP selective agonist DAMGO (E_{max} = 173%), proposing full agonist property. The efficacy measured for compound **6** was 162%, classifying it as an agonist of the MOP receptor.

Results of the enzymatic degradation study of the most potent analogues are summarized in Table 4. Compounds **2**

Table 4. Half-Lives of the EMs and Their Potent Analogues in a Crude Rat Brain Membrane Homogenate[a]

peptides	half-life (min)
1	5.8 ± 0.2
2	17 ± 0.9
3	34 ± 3
4	>1200
6	>1200

[a]Data are means of at least three individual experiments ± SEM. The protein content of the brain homogenate was 4.7 mg/mL. Half-lives were calculated on the basis of pseudo-first-order kinetics of the disappearance of the peptides.

and **3** demonstrated a moderately increased (3-fold and 6-fold, respectively) resistance against proteolytic enzymes in rat brain homogenate. Analogues containing alicyclic β-amino acids (compound **4** and **6**) have shown significantly prolonged half-lives compared to that of EM-2, suggesting enzymatic resistance. The obtained results confirmed that the insertion of alicyclic β-amino acids in the second position of EMs results in proteolytically stable analogues.[20]

Structure–Activity Studies. On the basis of their previously discussed biological properties, structural analysis was performed for compounds **2**, **3**, **4**, and **6**. NMR spectroscopic studies were done for compounds **2** and **3**. The ^{1}H NMR parameters such as chemical shifts (δ) of amide and aliphatic protons and intraresidue geminal (^2J) and vicinal (^3J) coupling constants are summarized in Table S1 (Supporting Information), and the ^{13}C chemical shifts of all protonated C-atoms are shown in Table S2 (Supporting Information). The ^{1}H NMR spectrum of both peptides contained two sets of signals indicating the presence of two conformational species. The structural difference between the two conformers is due to the *cis*/*trans* isomerization of the Tyr^1–Hyp^2 and Tyr^1–βPro^2 bonds as it was indicated by the distinctive pattern of ROESY

dx.doi.org/10.1021/jm300836n | J. Med. Chem. 2012, 55, 8418–8428

cross-peaks between H_α of Tyr[1] and H_α or $H_{\delta,\delta'}$ of Hyp[2] (compound **2**) and βPro[2] (compound **3**). The ratio of *cis* and *trans* isomers of compounds **2** and **3** was found to be approximately 1:5 and 1:3, respectively. The observed interresidue ROEs are illustrated in Figure 2 and listed in Table S3 (Supporting Information). Significantly more ROEs were observed for **3** than for **2**, and those observed for **3** included more crosspeaks corresponding to protons distant in the peptide sequence. This indicates that compound **3** adopts a more compact, folded structure at 315 K, while compound **2** remains relatively flexible even at 300 K. Rotamer populations of side chains of aromatic residues calculated from the vicinal proton−proton coupling constants $^3J_{H\alpha-H\beta}$ and $^3J_{H\alpha-H\beta'}$ (Table S1, Supporting Information) are summarized in Table 5. A slight preference for *gauche*− conformation was found for Phe[3] and Phe[4] residues in both compounds **2** and **3**. For the Tyr[1] side chain of compound **2** an approximately equal distribution of conformer populations was detected, while for compound **3**, the *trans* or *gauche*− rotameric state was found to be slightly higher than *gauche*+.

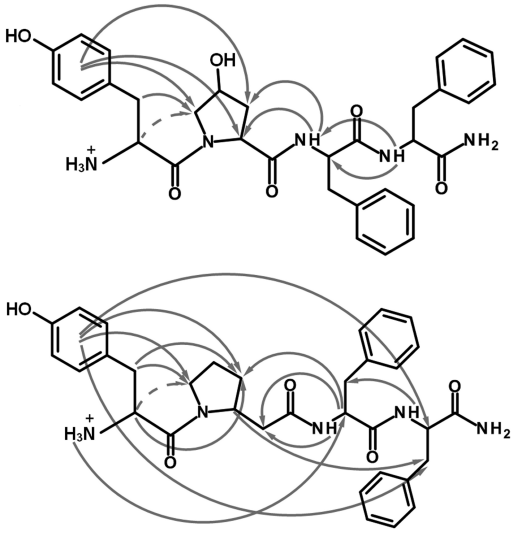

Figure 2. Chemical structure and main interresidue NOEs of compounds **2** (upper) and **3** (lower).

Structure refinement utilizing simulated annealing (SA), having NOE-derived proton−proton distances included as restraints, yielded 1000 member structural ensembles for compounds **2** and **3**. As a clear manifestation of ROESY results illustrated in Figure 2, compound **3** had shown a more pronounced tendency to form turn structures than compound **2** (Table 6). The fraction of *cis* Tyr[1]−Hyp[2] and Tyr[1]−βPro[2] peptide bonds was 5.9% and 11.6%, respectively, therefore the experimentally obtained approximate values of 17% and 25% were underestimated. Furthermore, a 2.6% population of *cis* βPro[2]−Phe[3] bond was also found among the refined structures of analogue **3**, although such isomerization was not detected by NMR. The populations of side chain rotameric states in the ensembles of refined structures (Table 5) were found to be strongly biased and to differ from those calculated from $^3J_{H\alpha-H\beta}$

Table 6. Occurrence of Bent Structures and Propensity of the Fulfillment of Pharmacophore Distance Criteria for Compounds 2, 3, 4, and 6 in H_2O and DMSO

method	peptide	occurrence of bent structure (%)	fulfillment of pharmacophore distance criteria (%)
SA	**2**	24.0	4.1
	3	50.8	0.0
MD in H_2O	**2**	14.7	10.1
	3	4.4	2.2
	4	80.0	7.2
	6	44.6	3.2
MD in DMSO	**2**	16.1	0.3
	3	5.9	4.1
	4	71.1	4.1
	6	69.0	5.1

Table 5. Rotamer Populations of Aromatic Side Chains in 2, 3, 4, and 6 in H_2O and DMSO

		rotamer populations (%)								
		Tyr[1]			Phe[3]			Phe[4]		
method	peptide	P(g−)	P(t)	P(g+)	P(g−)	P(t)	P(g+)	P(g−)	P(t)	P(g+)
NMR[a]	**2**	34	27	39	43	18	39	48	14	38
	3	19[b]	48[b]	33	66	9	25	49	13	38
SA	**2**	52.8	46.9	0.3	29.6	70.1	0.3	11.1	88.9	0.0
	3	97.9	0.0	2.1	90.8	9.2	0.0	75.3	24.7	0.0
MD in H_2O	**2**	13.0	79.8	7.2	25.9	40.7	33.4	34.7	22.7	42.6
	3	7.7	91.1	1.2	52.0	39.2	8.8	45.6	22.4	32.0
	4	37.9	57.5	4.6	6.3	86.0	7.7	7.2	90.7	2.1
	6	19.3	75.4	5.3	23.4	58.5	18.1	20.5	72.3	7.2
MD in DMSO	**2**	17.5	61.0	21.5	22.8	34.2	43.0	22.8	46.1	31.1
	3	17.7	75.7	6.6	48.3	36.3	15.4	30.0	24.2	45.8
	4	32.7	52.4	14.9	17.9	78.6	3.5	17.0	83.0	0.0
	6	40.0	55.0	5.0	26.5	69.0	4.5	32.0	65.6	2.4

[a]as determined from three-bond proton−proton ($J_{H\alpha-H\beta}$) coupling constants. Stereospecific assignment of β-protons was deduced from the ROE pattern. Populations are approximate (±10%) values. [b]interchangeable populations.

dx.doi.org/10.1021/jm300836n | J. Med. Chem. 2012, 55, 8418−8428

Table 7. Occurrence of Specific Intramolecular Hydrogen Bonds of Compounds 2, 3, 4, and 6, Expressed As Percentages of the Total Conformational Ensemble Generated by MD Simulations

		H_2O				DMSO			
hydrogen bond	stabilized structures[a]	2	3	4	6	2	3	4	6
CO(1)−−−HN(3)	γ-turns (A), C_8-turns (B)	1.1	0.2	0.6	<0.1	0.7	<0.1	1.2	<0.1
CO(2)−−−HN(4)	γ-turns (C)	1.6	0.1	0.5	2.8	4.0	<0.1	1.8	4.8
CO(1)−−−HN(4)	β-turns (D), C_{11}-turns (E)	7.4	0.8	1.2	0.5	5.0	1.7	5.2	1.1
CO(3)−−−HN(2)	C_9-turns (F)			<0.1	8.9			0.1	0.7
CO(4)−−−HN(2)	C_{12}-loops (G)			0.0	2.2			0.0	4.2
CO(1)−−−H_2N (C-term)	C_{13}- (H) and C_{14}-loops (I)	3.6	0.2	15.4	8.9	5.9	0.3	13.7	9.2
CO(2)−−−H_2N (C-term)	β-turns (J)	12.7	3.4	1.4	7.8	5.8	4.6	4.1	7.0
CO(3)−−−H_2N (C-term)	γ-turns (K)	0.1	<0.1	1.6	3.5	<0.1	0.1	1.7	11.8
NH_3^+(1)−−−OC(3)	C_{11}- and C_{12}-loops (L)	0.0	<0.1	24.0	8.6	0.0	0.0	27.4	0.1
NH_3^+(1)−−−OC(4)	N-to-C-terminal loops (M)	0.2	0.2	3.3	3.3	0.0	0.9	23.7	4.5

[a]Letters in parentheses refer to structures shown in Figure 3.

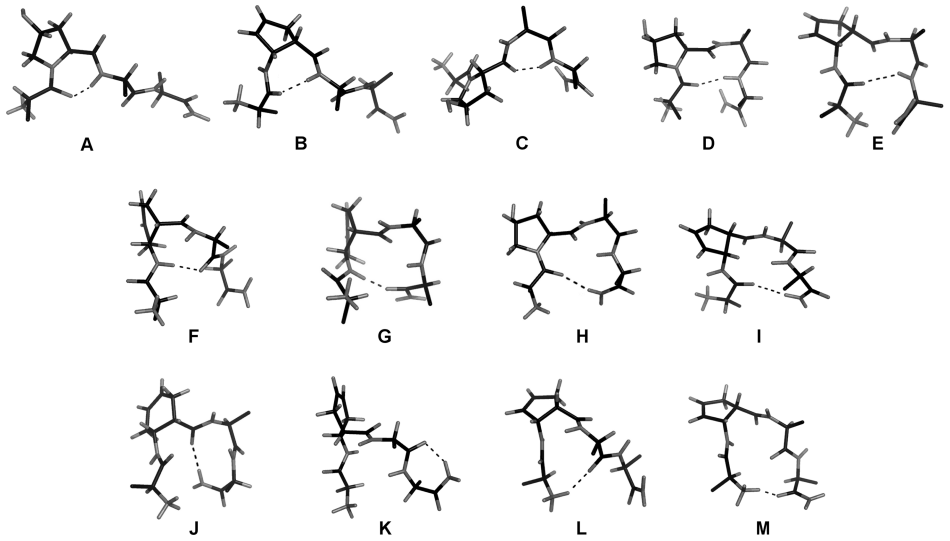

Figure 3. Examples of folded structures identified by the analysis of specific intramolecular hydrogen bonds: (A) γ-turn at Hyp^2 in **2**, (B) C_8-turn in **4**, (C) γ-turn at Phe^3 in **2**, (D) β-turn in **2**, (E) C_{11}-turn in **4**, (F) C_9-turn in **6**, (G) C-terminal C_{12}-loop in **6**, (H) C-terminal C_{13}-loop in **2**, (I) C-terminal C_{14}-loop in **4**, (J) C-terminal β-turn in **6**, (K) C-terminal γ-turn in **6**, (L) N-terminal C_{12}-loop in **4**, (M) N-to-C-terminal loop in **4**.

coupling constants. The fraction of structures which fulfill the previously proposed geometric criteria for the arrangement of pharmacophore groups[12] was found to be very low, even 0.0 in the case of compound **3**.

Molecular dynamics (MD) simulations and subsequent topographic analysis of trajectories indicated a strong preference for bent structures in the case of compounds **4** and **6**, both in H_2O and DMSO (Table 6). The occurrence of bent backbone structure was less dominant for compounds **2** and **3**. While in the case of compound **2** this fraction was close to that determined by SA structure refinement, for compound **3** the difference was much higher between the theoretical and the experimentally derived data. Note that average interproton distances calculated from MD results were found to match experimental ROE data (not shown). Analysis of specific intramolecular hydrogen bonds between all possible interacting pairs indicated various turn and loop structures which are presented in Table 7 and Figure 3. Several unique structural elements were identified for compounds **3**, **4**, and **6**, resulting from the elongation of the peptide backbone, similarly to that demonstrated previously for EM analogues containing saturated alicyclic β-amino acids.[18] Those structures are stabilized through hydrogen bonds and are analogous to the canonical secondary structural elements of peptides containing α-amino acids exclusively. Cluster analysis of the MD derived structural ensembles and inspection of the middle structures of the resultant clusters indicated the presence of different types of γ-, β-, and C_8-turns for all studied compounds (Table S4, Supporting Information), further dissecting the groups of possible structures identified by hydrogen bond analysis. Populations determined by cluster analysis are slightly underestimated in some cases when compared to data obtained from hydrogen bond analysis. Nevertheless, the sums of fractions of bent and turn structures were found to be approximately the same regardless of the method of analysis (topographic, hydrogen bond-based, or clustering) and the applied solvent environment. Apart from the single secondary structural elements listed in Tables 7 and S4 of the Supporting Information, the following combinations of structures were found: consecutive γ-turns (or C_8-turn + γ-turn) at positions 2 and 3, γ-turn (C_8-turn) at position 2 followed by a C-terminal β-turn, and a C_9-turn combined with a C-terminal β-turn. The side chain −OH group of Hyp^2 in compound **2** did not participate in any intramolecular hydrogen bonding. No specific structural element exclusively associated with *cis* Tyr^1−Xaa^2 peptide bond was found. Moreover, *cis* Tyr^1−Xaa^2 peptide

dx.doi.org/10.1021/jm300836n | J. Med. Chem. 2012, 55, 8418−8428

bonds were detected only in random/extended structures of compounds **2** and **3**. The only exception was the C-terminal β-turn of compound **3**, in which *cis* Tyr^1−Xaa^2 peptide bonds were found too. None of the identified specific secondary structural elements were found to correlate with receptor affinity. However, compounds of the desired bioactivity demonstrated high propensity of bent, folded backbone structure in general. No significant difference was found between populations of side chain conformational states in H_2O and DMSO environments (Table 5). However, results of MD simulations were found to deviate from those obtained from NMR data and SA structure refinement. For Tyr^1 of compounds **2** and **3**, a preference for *trans* conformation, while for Phe^3 and Phe^4 a relatively square distribution of rotameric states were detected. Only Phe^3 of compound **3** had shown a slight preference for *gauche*− conformation in H_2O. For compounds **4** and **6**, *trans* conformation was prevalent for all three aromatic side chains in both H_2O and DMSO, while the *gauche*+ conformation was the least preferred in most cases. Measurement of distances between the pharmacophore groups in structures along the trajectories indicated again that the studied compounds do not tend to conform to previously proposed criteria of MOP activity[12] (Table 6).

DISCUSSION

Receptor binding results and functional data obtained from [^{35}S]GTPγS binding experiments were in agreement with literature data in the case of compounds **2** and **3** and the parent ligand.[3,29,30] These results indicate that both the placement of a polar group on the Pro^2 side chain and the extension of the backbone by a $-CH_2-$ group, while preserving the tertiary amide moiety of Pro, has disadvantageous effects on MOP activity of EM-2 in general, regardless of different experimental conditions. However, the observed effect of βPro^2 substitution may not be applicable generally for all MOP ligands because, in a previous study, βPro-EM-1 exhibited MOP affinity, efficacy, and agonist behavior similar to those of DAMGO and EM-1.[35] This indicates that the incorporation of a $-CH_2-$ group between the pyrrolidine ring and the carboxyl group of the second residue of the EM sequence may affect receptor−ligand interactions differently when the following amino acid residue is Trp or Phe. Furthermore, diastereomeric βPro^2 substitution in morphiceptin yielded analogues with different biological activity profile, (*R*)βPro^2-morphiceptin, had higher MOP affinity than (*S*)βPro^2-morphiceptin.[30] This suggests that in certain cases MOP ligands may have distinct chiral requirements for the spacers between the biologically important Tyr and Phe residues. In EM analogues containing unsaturated alicyclic β-amino acids, the 1*S*,2*R* side chain configuration was shown to furnish MOP activity exclusively. This is in agreement with previous observations made for EM analogues containing the saturated variants of such residues.[20] Moreover, the modified side chain ring structure of ΔAcpc and ΔAchc was not proven to affect MOP binding because both receptor affinities and efficacies of compounds **4** and **6** were in the range of those of EM-2 and (1*S*,2*R*)$Acpc^2$/$Achc^2$−EM-2.

The resistance of compounds **4** and **6** against proteolytic degradation may be explained by the removal of the tertiary amide moiety by shifting the side chain ring along the backbone toward the C-terminus. Such an effect, previously observed in the case of $Acpc^2$/$Achc^2$-substituted EM analogues, was ascribed to the elongation of the side chain.[20] However, simple backbone extension by βPro^2-substitution in compound **3** had only decelerated digestion and failed to completely arrest the action of proteolytic enzymes. Incorporation of a polar side chain group in Pro^2 (compound **2**) provided similar results to that of compound **3**. Even though the catabolic breakdown of EM-2 is initiated by the cleavage of the Pro^2−Phe^3 peptide bond,[36] our results propose the tertiary amide moiety to be important in the recognition of EMs by specific proteolytic enzymes. The modification of this part of the molecule may be a fruitful strategy in the design of MOP ligands with enhanced in vivo stability, but the ability of the resultant compounds to cross the BBB and to present analgesic activity has to be assessed by performing in vivo experiments.

NMR studies were done for compounds which contain a tertiary amide moiety, therefore prone to *cis*−*trans* isomerization around that affected peptide bond. Experiments were done in DMSO-d_6, because this solvent has higher viscosity and lower relative permittivity than pure H_2O, hence it is a better approximation of the physical properties of intersynaptic fluids.[37] Compared to NMR data based on the integrated intensities of NH signals, the ratio of *cis*/*trans* isomers of the Tyr^1−Hyp^2/βPro^2 bonds was slightly underestimated by SA. This may be related to partial signal overlap in the NH region of ^{1}H NMR spectra, which makes it difficult to determine the accurate ratio of co-occurring conformers. The high propensity of bent, folded structures of compound **3**, suggested by NOE-restrained SA structure refinement studies, was not confirmed by MD simulation results. Furthermore, the distribution of side chain rotameric states of the refined structures did not agree with those calculated from $^3J_{H\alpha-H\beta}$ coupling constants. Nevertheless, the reliability of MD data was confirmed in all cases as the MD derived average interproton distances were found to be in agreement with experimental ROE data. This, together with our previous observations,[20] suggest that SA structure refinement employing ROE-derived distance restraints may not always be the best strategy, especially in the case of short, flexible peptides with fast rotating side chains where artifacts emerging from the low time resolution of NMR are utterly transmitted.

Apart from the justification given above for DMSO, the reason for running unrestrained MD simulations in both H_2O and DMSO solvents is to detect intrinsic conformational preferences which are independent of solvent environment. Secondary structural elements and the populations of side chain conformational states were shown to be fairly consistent in our MD simulation results regardless of the applied solvent, indicating that structural properties presented here are intrinsic properties of the studied molecules. Three different methods were applied for the secondary structural analysis in order to cross-compensate for their own specific limitations and provide a fairly accurate, general view of the solution conformational properties of compounds **2**, **3**, **4**, and **6**. A natural tendency to form bent structures was identified for the most potent EM analogues (compounds **4** and **6**). This is in agreement with numerous previous suggestions which emphasized the importance of such structures in MOP receptor binding.[13,16,18,19] No uniform agreement was found between the preferred side chain conformations of compounds **4** and **6** and those proposed by recent bioactive structure models. This suggests that for these molecules the optional arrangement of pharmacophore groups required for MOP binding and activation is formed as a result of binding.

Previously proposed distances between pharmacophore groups as a requirement for biological activity were measured

dx.doi.org/10.1021/jm300836n | J. Med. Chem. 2012, 55, 8418−8428

in a mainly unordered solution structure of morphiceptin and morphiceptin analogues possessing a *cis* Tyr[1]−Pro[2] peptide bond.[12] Since their introduction, the importance of these requirements was argued several times, as many potent MOP ligands were reported possessing different three-dimensional structures.[18] In addition, our study had also failed to identify a clear correlation between bioactivity and the fulfillment of pharmacophore distance criteria. Therefore we assume that these distances may be of less relevance than it was thought previously.

Besides acting as a spacer between pharmacophore groups of opioid peptides, Pro is well-known for its turn inducing effect in peptides and proteins. This effect is mainly attributed to the constrained ring structure and the tertiary amide moiety formed upon insertion into the peptide sequence. Our study indicated that Pro modifications which do not affect the aforementioned structural elements (Hyp, *β*Pro) may still decrease the propensity of turn structures in peptides. On the other hand, alicyclic *β*-amino acids were clearly shown to induce turn structure when built into an EM sequence to an extent exceeding Pro. As our analysis indicates, this may be due to the presence of a secondary instead of a tertiary amide moiety of which an NH group may participate in hydrogen bonds and further stabilize canonical and unique bent structures, while the rigid side chain ring structure orients the backbone similarly as Pro does. The structural and pharmacological properties of (1*S*, 2*R*)ΔAcpc[2]/ΔAchc[2]−EM-2 were found to be almost identical to those observed for the saturated variants, (1*S*, 2*R*)Acpc[2]/Achc[2]−EM-2.[20] This suggests that the modified puckering properties, introduced by the double bond in the side chain ring, do not have any different effect on the secondary structure of the incorporating tetrapeptide. In addition, care must be taken when ΔAcpc[2] or ΔAchc[2] substitutions are utilized to generate precursors for radioactive labeling or other chemical modifications of EM sequences because impurities consisting of the unreacted precursors may falsify in vitro pharmacological assay data. In addition to the deterministic structural effects discussed above, Pro[2] modifications may affect MOP receptor−ligand interactions directly through steric or electrostatic effects depending on the nature and degree of substitution. However, data presented here are not sufficient to provide basis for this latter speculation.

CONCLUSION

Systematic chemical modifications of Pro[2] of EM-2 provided us with potent MOP ligands (compounds **4** and **6**) with enhanced resistance against proteolytic enzymes abundant in rat brain tissue. The observed, exceptionally high metabolic stability is supposedly attributed to the replacement of the tertiary amide moiety in the backbone with a usual secondary amide bond by extension of the backbone and shifting the constrained ring structure toward the C-terminus. This modification was shown to preserve bioactivity depending on the configuration of the modified amino acid side chain. The most potent analogues were shown to adopt turn or bent structure with high propensity, advocating the importance of this structural arrangement, in agreement with numerous previous reports. However, solution conformational properties do not necessarily align with the bioactive structure in demand and the lack of an experimentally derived structural model of the MOP−peptide ligand complex as a reference makes it difficult to provide clear assumptions and comparisons. Nevertheless, identification of intrinsic conformational preferences supported by biological data may be relevant with regard to receptor−ligand interactions. Pro[2] is proposed to simply act as a "stereochemical spacer" in EMs. However, our results indicated, that Pro[2] and similar substituents are key participants in the shaping of the three-dimensional structure of the incorporating peptides. Pro[2] may take part in receptor−ligand interactions directly as a hydrophobic partner, however, this possibility needs further investigation.

EXPERIMENTAL SECTION

Chemicals. Fine chemicals of the best available grade were purchased from Sigma-Aldrich (St. Louis, MO, USA) unless stated otherwise. Boc-protected amino acids and 4-methylbenzhydralamine (MBHA) resin were purchased from Sigma-Aldrich or from Bachem Feinchemikalen AG (Bubendorf, Switzerland). Boc-*β*Pro was purchased from Polypeptide Group (Strasbourg, France). *cis*-(1*S*,2*R*/1*R*,2*S*)ΔAcpc and *cis*-(1*S*,2*R*/1*R*,2*S*)ΔAchc were generously provided by the research group of Prof. Ferenc Fülöp (University of Szeged, Hungary). 1-Hydroxybenzotrioazole (HOBt) and *N*,*N*-dicyclohexylcarbodiimide (DCC) coupling agents were purchased from Novabiochem (Läufelfingen, Switzerland) and Merck (Darmstadt, Germany), respectively. Acetonitrile and DMSO-d_6 was purchased from Merck and Cambridge Isotopes, respectively. [^{35}S]GTPγS (>1000 Ci/mmol) was obtained from Institute of Isotopes Co., Ltd. (Budapest, Hungary). [^{3}H]DAMGO (1.6 TBq/mmol, 43 Ci/mmol)[31] and [^{3}H] Ile^{5,6}-deltorophin-2 (1.5 TBq/mmol, 39 Ci/mmol)[38] were prepared in our laboratory from the appropriate halogenated peptide derivatives. The purity of final synthesis products was assessed by analytical RP-HPLC and found to be ≥96% in all cases.

Peptide Synthesis. Manual solid phase peptide synthesis was performed using similar protocol and reagents as described previously.[20] *cis*-(1*S*,2*R*/1*R*,2*S*)ΔAcpc and *cis*-(1*S*,2*R*/1*R*,2*S*)ΔAchc were incorporated in racemic form. The resin bound peptides were cleaved with anhydrous HF (10 mL/g resin) in the presence of anisole (1 mL/g resin) and dimethylsulfide (1 mL/g resin) at 0 °C for 60 min. All compounds were analyzed and separated by RP-HPLC. Analysis of all compounds was carried out by an Alltech Alltima (Grace, Columbia, MD, USA) analytic C_{18} reversed phase column (250 mm × 4.6 mm, 5 μm) with a flow rate of 1 mL/min. Separation of compounds was achieved on a Vydac (Grace, Columbia, MD, USA) 218TP1010 (250 mm × 10 mm, 12 μm) reversed phase column with a flow rate of 4 mL/min. The mobile phase was composed of 0.1% (v/v) TFA in water and 0.08% (v/v) TFA in acetonitrile, and 20 min linear gradient irrigations were carried out with 20% up to 60% organic modifier content. Mass spectra were recorded in the 50−990 Da range; the spectrometer was calibrated by using the MS/MS fragments of a 100 fmol [Glu^1]-fibrinopeptide B/μL solution. Analytical data of the resultant peptides are listed in Table 1.

Determination of the Configuration of (1*S*,2*R*/1*R*,2*S*)ΔAcpc and (1*S*,2*R*/1*R*,2*S*)ΔAchc in Peptides. Detailed description of the method is found elsewhere.[31,32] Briefly, 1 mg of peptide was hydrolyzed separately in 1 mL of 6 M HCl solution under nitrogen pressure for 24 h at 110 °C. GITC was added to the hydrolysis mixture in the presence of 0.8% triethylamine (TEA) in acetonitrile and allowed to react for 1 h at room temperature. After derivatization, the reaction mixture was analyzed by analytical RP-HPLC using the same instrumentation and conditions as described above. Peptide diastereomers were identified by comparison of retention factors to those obtained previously for these compounds.[31,32]

Rat Brain Membrane Preparation. The detailed procedure of the preparation of rat brain membrane homogenate was published elsewhere.[39] Rats (male, Wistar, 250−300 g body weight) were treated according to the European Communities Council Directives (86/609/ECC) and the Hungarian Act for the Protection of Animals in Research (1998/XXVIII. law, section IV.) The Bradford method was used to determine the protein content of the membrane preparation, using bovine serum albumin standard for calibration.[40]

Receptor Binding Assays. The detailed description of competition binding experiments was described previously.[41] Briefly,

heterologue competition binding experiments were performed by incubating rat brain membranes (0.2−0.5 mg protein/tube) with 1 nM [^{3}H] DAMGO for 1 h at 25 °C or 2 nM [^{3}H] Ile^{5,6}-deltorphin-2 for 45 min at 35 °C and 10^{-10}−10^{-5} M unlabeled ligands for MOP and DOP, respectively. Then 10 μM concentration of naloxone was used to measure the nonspecific bindings. Total binding was measured in the absence of ligand. Specific bindings were obtained by subtraction of nonspecific binding from the total binding. Inhibitory constants (K_i, [nM]) were calculated from the competition experiments by using nonlinear least-squares curve fitting and the Cheng−Prusoff equation[42] with GraphPad Prism software (version 4.0, San Diego, CA). Data are reported as means ± SEM of at least three independent measurements, each performed in duplicate.

Ligand-Stimulated [^{35}S]GTPγS Functional Binding Assay. The assay was performed according to the procedure described elsewhere.[39] Briefly, rat brain membranes (10−15 μg protein/tube) were incubated with 0.05 nM [^{35}S]GTPγS and 10^{-10}−10^{-5} M concentrations of unlabeled ligands in the presence of 30 μM GDP in Tris-EGTA buffer (50 mM Tris-HCl, 100 mM NaCl, 3 mM $MgCl_2$, and 1 mM EGTA, pH 7.4) at 30 °C for 60 min. Basal binding was determined in the absence of ligands and set at 100%. By using 10 μM unlabeled GTPγS, nonspecific binding was measured and subtracted from total binding. The percentage stimulation of the specific [^{35}S]GTPγS binding over the basal activity is reported as the mean ± SEM of at least three independent measurements. Each measurement was performed in triplicate and analyzed with the sigmoid dose−response curve-fitting option of the GraphPad Prism software to obtain potency (ED_{50}) and efficacy (E_{max}) values.

Metabolic Stability. The degradation studies of the endomorphin analogues were performed as described in detail earlier.[6] Briefly, peptide aliquots (20 μL of 1 mM stock solution in 50 mM Tris-HCl buffer, pH = 7.4) was digested with 180 μL of the rat brain homogenate (protein concentration: 4.7 mg/mL). The mixtures were incubated at 37 °C. From the incubation mixtures, 20 μL of aliquots were withdrawn and immediately acidified with 25 μL of 0.1 mM aqueous HCl solution to stop the degradation. Acidified mixtures were centrifuged (11340g, 5 min, 25 °C), and 10 μL of the obtained supernatant was analyzed by RP-HPLC on a Vydac 218TP54 analytical C_{18} reversed phase column using linear gradient 20% up to 60% over 20 min, mobile phase consisting of 0.1% (v/v) TFA in water and 0.08% (v/v) TFA in acetonitrile. By using least-squares linear regression analysis, the degradation rate constants (k) were determined using a minimum of five time points. Degradation half-lives ($t_{1/2}$) were calculated from the obtained rate constants as ln 2/k.

NMR Spectroscopy. Approximately 10 mg of compound **2** or **3** was dissolved in 0.5 mL of DMSO-d_6. NMR spectra of **2** and **3** were acquired at 300 and 315 K, respectively, by using an inverse multinuclear (bbi) single-axis gradient 5 mm probe. Proton and carbon chemical shifts were referenced to the solvent DMSO peak at 2.49 and 39.5 ppm, respectively. TOCSY and ROESY experiments were performed in phase-sensitive mode with mixing times of 60 and 150 ms, respectively. TOCSY spectra were acquired with 4096 data points in f_2 and 512 data points in f_1, and 16 scans were collected at each increment. The MLEV-17 mixing sequence was flanked by simultaneously switched spin-lock and gradient pulses to obtain the signals of pure absorption phase for coupling constant measurements.[43] ROESY spectra were recorded with 2048 data points in f_2 and 512 data points in f_1, and 64 scans were collected at each increment. The ^{1}H chemical shifts were assigned by following the standard protocol of Wüthrich[44] through 2D TOCSY[43] and ROESY experiments. The ^{13}C chemical shifts of protonated carbons were assessed on the basis of the gradient-enhanced HSQC experiment.[45] Proton−proton scalar coupling constants were measured from the 1D ^{1}H NMR and/or 2D TOCSY[43] spectra. In the latter case, the corresponding rows extracted from the TOCSY spectra were inversely Fourier transformed and then zero-filled to 16 K real data points. A Gaussian function was applied prior to the Fourier transform, and the final digital resolution of the resulting 1D traces was ∼0.3 Hz. The coupling constants $^3J_{H\alpha-H\beta}/^3J_{H\alpha-H\beta'}$ were used to estimate the population percentages of the three staggered rotamers around the $C_\alpha-C_\beta$ bond of the aromatic side chain groups utilizing the Pachler parametrization of the Karplus equation[46,47] with parameters appropriate for aromatic residues ($^{ap}J_{H\alpha-H\beta}$ = 13.9 Hz and $^{sc}J_{H\alpha-H\beta}$ = 3.55 Hz). The stereospecific assignment of β-protons was deduced from the ROE patterns. The volumes of ROESY crosspeaks were converted into distance bounds by using the intensities of the Hyp^2−H_δ,$H_{\delta'}$ and βPro^2−H_β,$H_{\beta'}$ peaks for calibration.

Structure Refinement. Three-dimensional structures of peptides **2** and **3** were generated at atomic resolution by simulated annealing (SA) using the AMBER 9 software package,[48] the AMBER ff99 force field parameter set,[49] and the GB/SA continuum solvation model.[50] Parameters for unnatural amino acid residues were supplemented from the generalized Amber force field (gAFF),[51] and partial charges were determined at the HF/6-31G(d) level using the restrained electrostatic potential (RESP) method. The nonbonded interaction energies were calculated between all atom pairs. Fully extended geometries of peptides **2** and **3** were used as starting structures for simulated annealing, and ROESY-derived interproton distances were included as restraints with a ± 10% tolerance interval. To avoid biasing the structures, only manually assigned, unambiguous ROESY crosspeaks were used, and ROEs fixing *cis* or *trans* conformation of peptide bonds were excluded from calculations. One annealing cycle started with gradual heating of the system from 0 to 1050 K in 20 ps, which was followed by equilibration at 1050 K for 50 ps and then 50 ps exponential cooling from 1050 to 50 K in 0.5 fs time steps. The temperature was regulated using the Langevin thermal model with a collision frequency of 2 ps^{-1}. The leapfrog algorithm was utilized for integration and bonds involving hydrogen atoms were constrained by the SHAKE algorithm. For each peptide the above annealing protocol was repeated 1000 times. Then 1000 steps of steepest descent, followed by 1500 steps of conjugate gradient minimization, was done for each of the resultant 1000 geometries in GB/SA environment, where the convergence criteria for the energy gradient was set at 10^{-4} kcal mol^{-1} Å and the long-range nonbonded interactions were calculated with no cutoff. The pool of minimized structures were probed for their backbone curvature, side chain conformations and the conformation of peptide bonds with the aid of analysis programs of the AMBER 9 and GROMACS 4.5.4[52] packages and Perl scripts written in-house.

Molecular Dynamics Simulations. Molecular dynamics (MD) simulations were performed for compounds **2**, **3**, **4**, and **6**. Starting geometries were generated by simulated annealing and subsequent energy minimization, following a similar protocol described above but excluding ROESY-derived distance restraints. For each peptide, 1000 structures were generated and the resultant pool of structures was clustered to identify different possible conformations. Clustering was performed with the g_cluster utility of the GROMACS 4.5.4 program package and the gromos[53] method with a 0.5 Å rmsd similarity cutoff, fitting main chain and C_β atoms. Middle structures of the resultant clusters were analyzed one by one by using the Pymol (DeLano Scientific, version 0.99rc6)[54] molecular visualization and analysis program. For peptides **2** and **3**, six markedly different, dominant conformations were found, while for compounds **4** and **6**, five conformations were selected as starting structures for MD simulations. The Tyr^1−ΔAcpc^2 and Tyr^1−ΔAchc^2 peptide bonds of peptides **4** and **6** were set to *trans* conformation in all selected starting geometries, reflecting observations made previously for this family of compounds.[20] In the case of peptides **2** and **3**, the ratio of starting conformers, possessing *cis* or *trans* Tyr^1−Hyp^2 and Tyr^1−βPro^2 peptide bonds, was set to reflect results obtained from NMR spectroscopic studies. MD simulations of each selected starting structure of the four compounds were executed using the GROMACS 4.5.4 program package and the same force field parameters as described above. Each starting structure was immersed in a cubic box (35 Å × 35 Å × 35 Å) of pre-equilibrated TIP3P[55] water or DMSO[56] molecules. Solvent molecules were removed from the box when the distance between any atom of the solute molecule and any atom of the solvent molecule was less than the sum of the van der Waals radii of both atoms. Charged *N*-termini of peptides were neutralized by replacing solvent molecules by Cl^- ions at the positions of the first

dx.doi.org/10.1021/jm300836n | J. Med. Chem. 2012, 55, 8418−8428

solvent molecule with the most favorable electrostatic potential. All systems were then subjected to 1000 steps of steepest descent energy minimization with convergence criteria of 0.001 kJ mol^{-1}. Subsequently, peptides were subjected to 100 ps NVT MD at 300 K, fixing the position of the solute in the center of the box with a force constant of 1000 kJ mol^{-1} $Å^2$ on each heavy atom to allow the solvent density to equilibrate around the solute molecule. Then 50.25 ns NPT MD simulations were performed for the six starting geometries of **2** and **3**, while each of the five starting conformations appointed to compounds **4** and **6** were simulated for 60.25 ns at constant temperature (300 K) and pressure (1 bar) with the following parameters: the time step was set to 2 fs, the LINCS algorithm was used to constrain all bonds to their correct lengths, temperature was regulated with the v-rescale algorithm with a coupling constant of 0.1 ps, and constant pressure was maintained using isotropic scaling with a relaxation constant of 1.0 ps and 4.5×10^{-5} bar^{-1} and 5.25×10^{-5} bar^{-1} isothermal compressibility for water and DMSO, respectively. Nonbonded interactions were calculated using the PME method with all cutoff values set at 10 Å. The coordinates were stored after every 10 steps to yield a total of 25000−30000 sampled conformations for each trajectory after excluding the first 0.25 ns, which was regarded as equilibration. The trajectories resulting from these five or six different initial conformations were then combined to yield 300 ns long trajectories of 150000 sampled conformations for each peptide.

The peptide structures along each trajectory were analyzed with the analysis programs of the GROMACS 4.5.4 program suite and Perl scripts written in-house. Three independent methods were applied to identify secondary structure and dominant conformational states. First, trajectories were probed for the existence of intramolecular hydrogen bonds by the g_hbond utility of GROMACS 4.5.4. The cutoff distance between a donor and an acceptor atom was set to 3.5 Å, and 60° was used as the cutoff for the donor−hydrogen−acceptor angle. Second, clustering of structural ensembles was performed as described earlier but with a 1 Å rmsd similarity cutoff. Every fifteenth backbone coordinate set from the trajectories was included in the analysis, which resulted in 15000 × 15000 rmsd matrices. Third, the backbone structure was examined through measurement of the C(1)−C_α(2)−C_α(3)−N(4) virtual dihedral angle and the distance between the terminal C_α atoms. A bend structure was assigned when this dihedral angle was between −80° and 80°, and the distance was less than 10.0 Å.[57] The distances between the putative pharmacophore elements and side chain rotamer populations were also determined.

■ ASSOCIATED CONTENT

Ⓢ Supporting Information

^{1}H NMR chemical shifts and coupling constants, ^{13}C NMR chemical shifts and ROE assignments for compounds **2** and **3**; frequency of secondary structural elements determined by cluster analysis; analytical RP-HPLC chromatograms of the final, purified peptides. This material is available free of charge via the Internet at http://pubs.acs.org

■ AUTHOR INFORMATION

Corresponding Author

*Phone: (+36) 62 599-647. E-mail: geza@brc.hu.

Notes

The authors declare no competing financial interest.

■ ACKNOWLEDGMENTS

We thank Prof. Ferenc Fülöp for providing the alicylic β-amino acid building blocks for peptide synthesis. For Jayapal Reddy Mallareddy, a six-month research scholarship was generously provided by the Foundation for the Hungarian Peptide and Protein Research. Financial support from the Hungarian Scientific Research Fund (OTKA CK-77515) and TÁMOP-4.2.1./B-09/1/KONV-2010-0007 are acknowledged.

■ ABBREVIATIONS USED[a]

Acpc, 2-aminocyclopentane-1-carboxylic acid; Achc, 2-aminocyclohexane-1-carboxylic acid; ΔAcpc, 2-aminocyclopentene-1-carboxylic acid; ΔAchc, 2-aminocyclohexene-1-carboxylic acid; Aze, (*S*)-azitidine-2-carboxylic acid; 3Aze, (*R*)-azitidine-3-carboxylic acid; BBB, blood−brain barrier; Boc, N_α-*tert*-butyloxycarbonyl; βPro, (*S*)-β-homoproline; CNS, central nervous system; DAMGO, H-Tyr-D-Ala-Gly-NMePhe-Gly-ol; $Ile^{5,6}$-deltorphin-2, H-Tyr-D-Ala-Phe-Glu-Ile-Ile-Gly-NH_2; DCC, *N*,*N*-dicyclohexylcarbodiimide; DCM, dichloromethane; DIEA, diisopropylethylamine; DOP, δ-opioid receptor; DMSO, dimethylsulfoxide; Dmt, 2′,6′-dimethyltyrosine; EGTA, ethylene glycol-bis(2-aminoethyl ether)-*N*,*N*,*N*,*N*-tetraacetic acid; EM-1, H-Tyr-Pro-Trp-Phe-NH_2; EM-2, H-Tyr-Pro-Phe-Phe-NH_2; GB/SA, generalized Born/solvent accessible surface; GITC, 2,3,4,6-tetra-*O*-acetyl-β-glucopyranosyl isothiocyanate; GDP, guanosine-5′-diphosphate; GTPγS, guanosine-5′-*O*-(3-thio)triphosphate; GPCR, G-protein-coupled receptor; HOBt, 1-hydroxybenzotrioazole; HRMS, high resolution mass spectrometry; HSQC, heteronuclear single quantum correlation; Hyp, (2*S*,4*R*)-4-hydroxypyrrolidine-2-carboxylic acid; KOP, κ-opioid receptor; MOP, μ-opioid receptor; MBHA, 4-methylbenzhydrylamine; MALDI-TOF, matrix-assisted laser desorption/ionization-time-of-flight; MD, molecular dynamics; NMR, nuclear magnetic resonance spectroscopy; NOE, nuclear Overhauser effect; PME, particle-mesh Ewald; ψPro, pseudoproline; RESP, restrained electrostatic potential; ROESY, rotating-frame Overhauser effect spectroscopy; RP-HPLC, reversed-phase high-performance liquid chromatography; SA, simulated annealing; SEM, standard error of the mean; TEA, triethylamine; Tris, 2-amino-2-hydroxymethyl-propane-1,3-diol; TFA, trifluoroacetic acid; Tic, 1,2,3,4-tetrahydroisoquinoline-3-carboxylic acid; TLC, thin-layer chromatography; TOCSY, total correlation spectroscopy

■ ADDITIONAL NOTE

[a]These abbreviations and definitions are in line with those recommended by the IUPAC-IUB Commission of Biochemical Nomenclature.

■ REFERENCES

(1) Janecka, A.; Fichna, J.; Janecki, T. Opioid receptors and their ligands. *Curr. Top. Med. Chem.* **2004**, *4*, 1−17.

(2) Reisine, T.; Bell, G. I. Molecular biology of opioid receptors. *Trends Neurosci.* **2004**, *16*, 506−510.

(3) Zadina, J. E.; Hackler, L.; Ge, L. J.; Kastin, A. J. A potent and selective endogenous agonist for the mu-opiate receptor. *Nature* **1997**, *386*, 499−502.

(4) Hackler, L.; Zadina, J. E.; Ge, L. J.; Kastin, A. J. Isolation of relatively large amounts of endomorphin-1 and endomorphin-2 from human brain cortex. *Peptides* **1997**, *18*, 1635−1639.

(5) Shane, R.; Wilk, S.; Bodnar, R. J. Modulation of endomorphin-2-induced analgesia by dipeptidyl peptidase IV. *Brain Res.* **1999**, *815*, 278−286.

(6) Tömböly, C.; Péter, A.; Tóth, G. In vitro quantitative study of the degradation of endomorphins. *Peptides* **2002**, *23*, 1573−1580.

(7) Hau, V. S.; Huber, J. D.; Campos, C. R.; Lipkowski, A. W.; Misicka, A.; Davis, T. P. Effect of guanidino modification and proline substitution on the in vitro stability and blood−brain barrier permeability of endomorphin II. *J. Pharm. Sci.* **2002**, *91*, 2140−2149.

(8) Gentilucci, L.; Tolomelli, A. Recent advances in the investigation of the bioactive conformation of peptides active at the mu-opioid receptor: conformational analysis of endomorphins. *Curr. Top. Med. Chem.* **2004**, *4*, 105−121.

(9) Janecka, A.; Kruszynski, R. Conformationally restricted peptides as tools in opioid receptor studies. *Curr. Med. Chem.* **2005**, *12*, 471−481.
(10) Keresztes, A.; Borics, A.; Tóth, G. Recent Advances in endomorphin engineering. *ChemMedChem* **2010**, *5*, 1176.
(11) Leitgeb, B. Structural investigation of endomorphins by experimental and theoretical methods: hunting for the bioactive conformation. *Chem. Biodiversity* **2007**, *4*, 2703−2724.
(12) Yamazaki, T.; Ro, S.; Goodman, M.; Chung, N. N.; Schiller, P. W. A topochemical approach to explain morphiceptin bioactivity. *J. Med. Chem.* **1993**, *36*, 708−719.
(13) Kazmierski, W. D.; Ferguson, R. D.; Lipkowski, A. W.; Hruby, V. J. A topographical model of mu-opioid and brain somatostatin receptor selective ligands. NMR and molecular dynamics studies. *Int. J. Pept. Protein Res.* **1995**, *46*, 265−278.
(14) Podlogar, B. L.; Paterlini, M. G.; Ferguson, D. M.; Leo, G. C.; Demeter, D. A.; Brown, F. K.; Reitz, A. B. Conformational analysis of the endogenous mu-opioid agonist endomorphin-1 using NMR spectroscopy and molecular modeling. *FEBS Lett.* **1998**, *439*, 13−20.
(15) Keller, M.; Boissard, C.; Patiny, L.; Chung, N. N.; Lemieux, C.; Mutter, M.; Schiller, P. W. Pseudoproline-containing analogues of morphiceptin and endomorphin-2: evidence for a cis Tyr-Pro amide bond in the bioactive conformation. *J. Med. Chem.* **2001**, *44*, 3896−3903.
(16) Eguchi, M.; Shen, R. Y. W.; Shea, J. P.; Lee, M. S.; Kahn, M. Design, synthesis, and evaluation of opioid analogues with non-peptidic beta-turn scaffold: enkephalin and endomorphin mimetics. *J. Med. Chem.* **2002**, *45*, 1395−1398.
(17) Martinek, T. A.; Ötvös, F.; Dervarics, M.; Tóth, G.; Fülöp, F. Ligand-based prediction of active conformation by 3D-QSAR flexibility descriptors and their application in 3 + 3D-QSAR models. *J. Med. Chem.* **2005**, *48*, 3239−3250.
(18) Borics, A.; Tóth, G. Structural comparison of mu-opioid receptor selective peptides confirmed four parameters of bioactivity. *J. Mol. Graphics Modell.* **2010**, *28*, 495−505.
(19) Gentilucci, L.; Tolomelli, A.; De Marco, R.; Spampinato, S.; Bedini, A.; Artali, R. The inverse type II β-turn on D-Trp-Phe, a pharmacophoric motif for MOR agonists. *ChemMedChem.* **2011**, *6*, 1640−1653.
(20) Keresztes, A.; Szűcs, M.; Borics, A.; Kövér, K. E.; Forró, E.; Fülöp, F.; Tömböly, Cs.; Péter, A.; Páhi, A.; Fábián, G.; Murányi, M.; Tóth, G. New endomorphin analogues containing alicyclic beta-amino acids: influence on bioactive conformation and pharmacological profile. *J. Med. Chem.* **2008**, *51*, 4270−4279.
(21) Tömböly, Cs.; Ballet, S.; Feytens, D.; Kövér, K. E.; Borics, A.; Lovas, S.; Al-Khrasani, M.; Fürst, Z.; Tóth, G.; Benyhe, S.; Tourwé, D. Endomorphin-2 with a beta-turn backbone constraint retains the potent mu-opioid receptor agonist properties. *J. Med. Chem.* **2008**, *51*, 173−177.
(22) Manglik, A.; Kruse, A. C.; Kobilka, T. S.; Thian, F. S.; Mathiesen, J. M.; Sunahara, R. K.; Pardo, L.; Weis, W. I.; Kobilka, B. K.; Granier, S. Crystal structure of the μ-opioid receptor bound to a morphinan antagonist. *Nature* **2012**, *485*, 321−326.
(23) Schiller, P. W.; Weltrowska, G.; Berezowska, I.; Nguyen, T. M.; Wilkes, B. C.; Lemieux, C.; Chung, N. N. The TIPP opioid peptide family: development of delta antagonists, delta agonists, and mixed mu agonist/delta antagonists. *Biopolymers* **1999**, *51*, 411−425.
(24) Perlikowska, R.; Gach, K.; Fichna, J.; Toth, G.; Walkowiak, B.; do-Rego, J. C.; Janecka, A. Biological activity of endomorphin and [Dmt^1]endomorphin analogs with six-membered proline surrogates in position 2. *Bioorg. Med. Chem.* **2009**, *17*, 3789−3794.
(25) Torino, D.; Mollica, A.; Pinnen, F.; Lucente, G.; Feliciani, F.; Davis, P.; Lai, J.; Ma, S. W.; Porreca, F.; Hruby, V. J. Synthesis and evaluation of new endomorphin analogues modified at the Pro(2) residue. *Bioorg. Med. Chem. Lett.* **2009**, *19*, 4115−4118.
(26) Casy, A. F. *The Steric Factor in Medicinal Chemsitry: Dissymetric Probes of Pharmacological Receptors*; Plenum Press: New York, 1993.
(27) Paterlini, M. G.; Avitable, F.; Ostrowski, B. G.; Ferguson, D. M.; Portoghese, P. S. Stereochemical requirements for receptor recognition of the μ-opioid peptide endomorphin-1. *Biophys. J.* **2000**, *78*, 590−599.
(28) Gorres, K. L.; Raines, R. T. Prolyl 4-hydroxylase. *Crit. Rev. Biochem. Mol. Biol.* **2010**, *45*, 106−124.
(29) Biondi, B.; Giannini, E.; Negri, L.; Melchiorri, P.; Lattanzi, R.; Rosso, F.; Ciocca, L.; Rocchi, R. Opioid Peptides: Synthesis and Biological Activity of New Endomorphin Analogues. *Int. J. Pept. Res. Ther.* **2006**, *12*, 145−151.
(30) Giordano, C.; Sansone, A.; Masi, A.; Lucente, G.; Punzi, P.; Mollica, A.; Pinnen, F.; Feliciani, F.; Cacciatore, I.; Davis, P.; Lai, J.; Ma, S. W.; Porreca, F.; Hruby, V. J. Synthesis and activity of endomorphin-2 and morphiceptin analogues with proline surrogates in position 2. *Eur. J. Med. Chem.* **2010**, *45*, 4594−4600.
(31) Péter, A.; Fülöp, F. High-performance liquid chromatoraphic method for the separation of isomers of *cis*- and *trans*-2-amino-cyclopentane-1-carboxylic acid. *J. Chromatogr., A* **1995**, *715*, 219−226.
(32) Keresztes, A.; Tóth, G.; Fülöp, F.; Szűcs, M. Synthesis, radiolabeling and receptor binding of [^{3}H][(1*S*,2*R*)ACPC^2]-endomorphin-2. *Peptides* **2006**, *27*, 3315−3321.
(33) Handa, B. K.; Land, A. C.; Lord, J. A.; Morgan, B. A.; Rance, M. J.; Smith, C. F. Analogues of beta-LPH61−64 possessing selective agonist activity at mu-opiate receptors. *Eur. J. Pharmacol.* **1981**, *70*, 531−540.
(34) Hosohata, K.; Burkey, T. H.; Alfaro-Lopez, J.; Varga, E.; Hruby, V. J.; Roeske, W. R.; Yamamura, H. I. Endomorphin-1 and endomorphin-2 are partial agonists at the human mu-opioid receptor. *Eur. J. Pharmacol.* **1998**, *346*, 111−114.
(35) Cardillo, G.; Gentilucci, L.; Qasem, A. R.; Sgarzi, F.; Spampinato, S. Endomorphin-1 analogues containing beta-proline are mu-opioid receptor agonists and display enhanced enzymatic hydrolysis resistance. *J. Med. Chem.* **2002**, *45*, 2571−2578.
(36) Mentlein, R. Dipeptidyl-peptidase IV (CD26)—role in the inactivation of regulatory peptides. *Regul. Pept.* **1999**, *85*, 9−24.
(37) Albrizio, S.; Carotenuto, A.; Fattorusso, C.; Moroder, L.; Picone, D.; Temussi, P. A.; D'Ursi, A. Environmental mimic of receptor interaction: conformational analysis of CCK-15 in solution. *J. Med. Chem.* **2002**, *45*, 762−769.
(38) Nevin, S. T.; Kabasakal, L.; Ötvös, F.; Tóth, G.; Borsodi, A. Binding characteristics of the novel highly selective delta agonist, [3H]IIe5,6deltorphin II. *Neuropeptides* **1994**, *26*, 261−265.
(39) Fábián, G.; Bozó, B.; Szikszay, M.; Horváth, G.; Coscia, C. J.; Szücs, M. Chronic morphine-induced changes in mu-opioid receptors and G proteins of different subcellular loci in rat brain. *J. Pharmacol. Exp. Ther.* **2002**, *302*, 774−780.
(40) Bradford, M. M. A rapid and sensitive method for the quantitation of microgram quantities of protein utilizing the principle of protein−dye binding. *Anal. Biochem.* **1976**, *72*, 248−254.
(41) Bozó, B.; Fülöp, F.; Tóth, G. K.; Tóth, G.; Szücs, M. Synthesis and opioid binding activity of dermorphin analogues containing cyclic beta-amino acids. *Neuropeptides* **1997**, *31*, 367−372.
(42) Cheng, Y.; Prusoff, W. H. Relationship between the inhibition constant (K1) and the concentration of inhibitor which causes 50% inhibition (I50) of an enzymatic reaction. *Biochem. Pharmacol.* **1973**, *22*, 3099−3108.
(43) Kövér, K. E.; Uhrin, D.; Hruby, V. J. Gradient- and Sensitivity-Enhanced TOCSY Experiments. *J. Magn. Reson.* **1998**, *130*, 162−168.
(44) Wüthrich, K. *NMR of Proteins and Nucleic Acids*; Wiley: New York, 1986.
(45) Schleucher, J.; Schwendinger, M.; Sattler, M.; Schmidt, P.; Schedletzky, O.; Glaser, S. J.; Sorensen, O. W.; Griesinger, C. A general enhancement scheme in heteronuclear multidimensional NMRemploying pulsed field gradients. *J. Biomol. NMR* **1994**, *4*, 301−306.
(46) Pachler, K. G. R. Nuclear Magnetic Resonance Study of Some Alpha-Amino Acids. 1. Coupling Constants in Alkaline and Acidic Medium. *Spectrochim. Acta* **1963**, *19*, 2085−2092.
(47) Pachler, K. G. R. Nuclear Magnetic Resonance Study of Some Alpha-Amino Acids-II. Rotational isomerism. *Spectrochim. Acta* **1964**, *20*, 581−587.

(48) Case, D. A.; Darden, T. A.; Cheatham, T. E.; Simmerling, C. L.; Wang, J.; Duke, R. E.; Luo, R.; Merz, K. M.; Pearlman, D. A.; Crowley, M.; Walker, R. C.; Zhang, W.; Wang, B.; Hayik, S.; Roitberg, A.; Seabra, G.; Wong, K. F.; Paesani, F.; Wu, X.; Brozell, S.; Tsui, V.; Gohlke, H.; Yang, L.; Tan, C.; Mongan, L.; Hornak, V.; Cui, G.; Beroza, P.; Matthews, D. H.; Schafmeister, C.; Ross, W. S.; Kollman, P. A. *AMBER 9*; University of California: San Francisco, 2006.
(49) Wang, J.; Cieplak, P.; Kollman, P. A. How well does a restrained electrostatic potential (RESP) model perform in calculating conformational energies of organic and biological molecules? *J. Comput. Chem.* **2000**, *21*, 1049−1074.
(50) Still, W. C.; Tempczyk, A.; Hawley, R. C.; Hendrickson, T. S. Semianalytical treatment of solvation for molecular mechanics and dynamics. *J. Am. Chem. Soc.* **1990**, *112*, 6127−6129.
(51) Wang, J.; Wolf, R. M.; Caldwell, J. W.; Kollman, P. A. Development and testing of a general Amber force field. *J. Comput. Chem.* **2004**, *25*, 1157−1174.
(52) van der Spoel, D.; Lindahl, E.; Hess, B.; Groenhof, G.; Mark, A. E.; Berendsen, H. J. C. GROMACS: Fast, Flexible, and Free. *J. Comput. Chem.* **2005**, *26*, 1701−1718.
(53) Daura, X.; Gademann, K.; Jaun, B.; Seebach, D.; van Gunsteren, W. F.; Mark, A. E. Peptide folding: when simulation meets experiment. *Angew. Chem., Int. Ed.* **1999**, *38*, 236−240.
(54) DeLano, W. L. *The PyMOL Molecular Graphics System*; DeLano Scientific LLC: San Carlos, CA, 2002; http://www.pymol.org.
(55) Jorgensen, W. L.; Chandrasekhar, J.; Madura, J.; Klein, M. L. Comparison of simple potential functions for simulating liquid water. *J. Chem. Phys.* **1983**, *79*, 926−935.
(56) Fox, T.; Kollman, P. A. Application of the RESP methodology in the parametrization of organic solvents. *J. Phys. Chem. B* **1998**, *102*, 8070−8079.
(57) Ball, J. B.; Hughes, R. A.; Alewood, P. F.; Andrews, P. R. β-Turn topography. *Tetrahedron* **1993**, *49*, 3467−3478.